Correction

NEUROSCIENCE

Correction for "Cocaine elicits autophagic cytotoxicity via a nitric oxide-GAPDH signaling cascade," by Prasun Guha, Maged M. Harraz, and Solomon H. Snyder, which appeared in issue 5, February 2, 2016, of *Proc Natl Acad Sci USA* (113:1417–1422; first published January 19, 2016; 10.1073/pnas.1524860113).

The authors note that Fig. 1 appeared incorrectly. The corrected figure and its legend appear below.

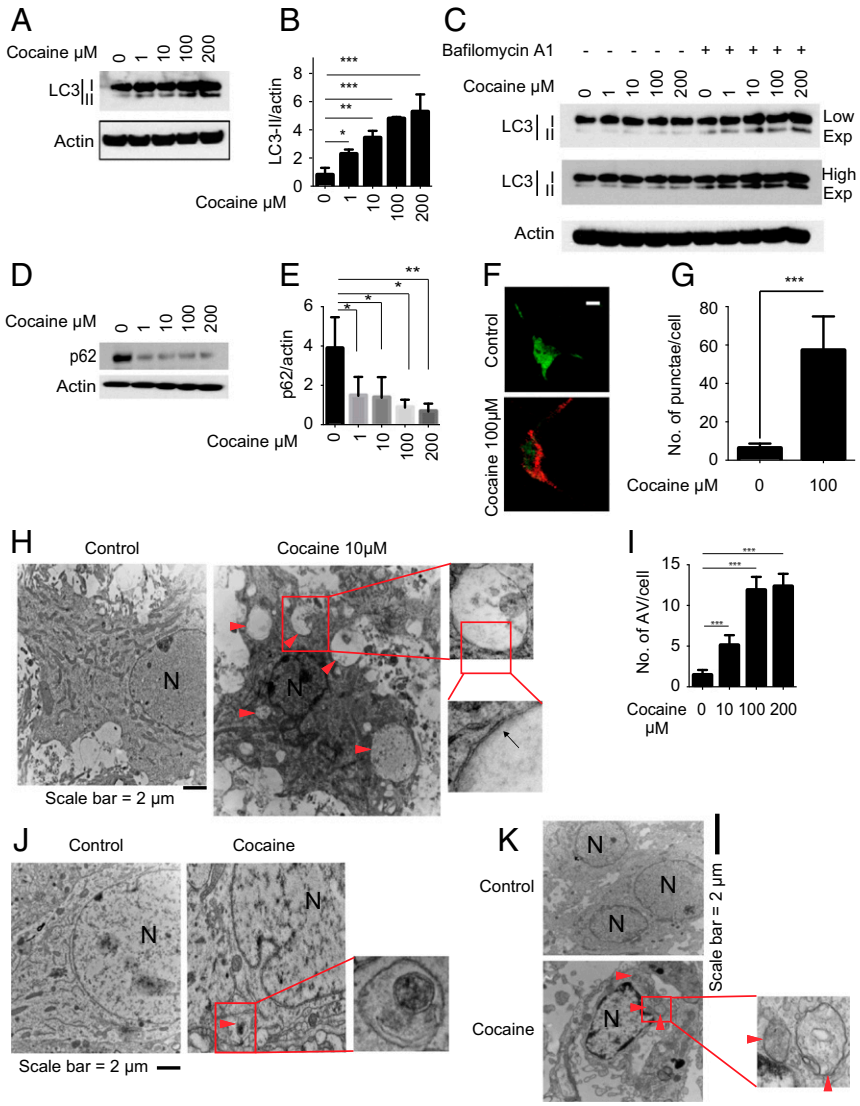

Fig. 1. Cocaine elicits autophagy in neuronal system. (*A* and *B*) Immunoblots and quantification assessing the protein levels of LC3-II in response to indicated concentrations of cocaine in cortical cultures ($n = 3$). (*C*) Immunoblot assessing the protein levels of LC3-II in response to indicated concentrations of cocaine ±100 nM bafilomycin-A1. (*D*) Immunoblots assessing the protein levels of p62 in response to indicated concentrations of cocaine in cortical cultures. (*E*) Quantification of p62 protein levels in response to cocaine in cortical cultures ($n = 3$). (*F*) Confocal imaging of LC3 puncta (red) in cortical neurons ± 100 μM cocaine. Neuronal nuclei were stained green with NeuN antibody. (*G*) Quantification of LC3-II puncta per neuron ± cocaine treatment. A total of 50 neurons were counted. (Scale bar: 10 μm.) Data are represented as mean ± SD; ***$P < 0.001$, one-way ANOVA. (*H*) Transmission electron microscopy (TEM) images of cortical neurons with different indicated concentrations of cocaine for 3 h. Arrowhead represents autophagic vesicle, N denotes nucleus. (Scale bar: 2 μm.) The red boxed area contains a representative autophagic vacuole at 25,000× magnification. Arrow indicates double membrane of autophagic vacuole at 60,000× magnification. (*I*) Quantification of autophagic vacuoles per neuron ± cocaine. A total of 30 neurons were counted. Data are represented as mean ± SD; ***$P < 0.001$, **$P < 0.01$, *$P < 0.05$, one-way ANOVA. (*J*) TEM images of adult brain lateral habenula injected with vehicle or 20 mg/kg cocaine (intraperitoneal) for 3 h. (Scale bar: 2 μm.) The red boxed area contains a representative autophagic vacuole at 60,000× magnification. (*K*) TEM images of mouse fetal brain cerebral cortex. Timed pregnant mice were injected with vehicle or 20mg/kg cocaine (intraperitoneal) for 3 h. (Scale bar: 2 μm.) The red boxed area contains representative autophagic vacuoles at 60,000× magnification.

www.pnas.org/cgi/doi/10.1073/pnas.1700995114

Cocaine elicits autophagic cytotoxicity via a nitric oxide-GAPDH signaling cascade

Prasun Guha[a,1], Maged M. Harraz[a,1], and Solomon H. Snyder[a,b,c,2]

[a]The Solomon H. Snyder Department of Neuroscience, Johns Hopkins University School of Medicine, Baltimore, MD 21205; [b]Department of Psychiatry and Behavioral Sciences, Johns Hopkins University School of Medicine, Baltimore, MD 21205; and [c]Department of Pharmacology and Molecular Sciences, Johns Hopkins University School of Medicine, Baltimore, MD 21205

Contributed by Solomon H. Snyder, December 21, 2015 (sent for review November 10, 2015; reviewed by Ronald S. Duman and Eric J. Nestler)

Cocaine exerts its behavioral stimulant effects by facilitating synaptic actions of neurotransmitters such as dopamine and serotonin. It is also neurotoxic and broadly cytotoxic, leading to overdose deaths. We demonstrate that the cytotoxic actions of cocaine reflect selective enhancement of autophagy, a process that physiologically degrades metabolites and cellular organelles, and that uncontrolled autophagy can also lead to cell death. In brain cultures, cocaine markedly increases levels of LC3-II and depletes p62, both actions characteristic of autophagy. By contrast, cocaine fails to stimulate cell death processes reflecting parthanatos, monitored by cleavage of poly(ADP ribose)polymerase-1 (PARP-1), or necroptosis, assessed by levels of phosphorylated mixed lineage kinase domain-like protein. Pharmacologic inhibition of autophagy protects neurons against cocaine-induced cell death. On the other hand, inhibition of parthanatos, necroptosis, or apoptosis did not change cocaine cytotoxicity. Depletion of ATG5 or beclin-1, major mediators of autophagy, prevents cocaine-induced cell death. By contrast, depleting caspase-3, whose cleavage reflects apoptosis, fails to alter cocaine cytotoxicity, and cocaine does not alter caspase-3 cleavage. Moreover, depleting PARP-1 or RIPK1, key mediators of parthanatos and necroptosis, respectively, did not prevent cocaine-induced cell death. Autophagic actions of cocaine are mediated by the nitric oxide-glyceraldehyde-3-phosphate dehydrogenase signaling pathway. Thus, cocaine-associated autophagy is abolished by depleting GAPDH via shRNA; by the drug CGP3466B, which prevents GAPDH nitrosylation; and by mutating cysteine-150 of GAPDH, its site of nitrosylation. Treatments that selectively influence cocaine-associated autophagy may afford therapeutic benefit.

cocaine | autophagy | cell death | nitric oxide | GAPDH

Cocaine is a well recognized behavioral stimulant, which is widely abused. Its behavioral effects are thought to reflect inhibition of the reuptake inactivation of biogenic amines, especially serotonin and dopamine (1–4). Transcriptional regulation may underlie long-term effects of cocaine, especially the transition from abuse to addiction (5–12). Cocaine is also notably neurotoxic and broadly cytotoxic, but mechanisms for such actions have not been well characterized. Diverse modes of cytotoxicity and cell death have been delineated (13). Apoptosis is well established as a programmed form of cell death (14, 15). Earlier work had regarded necrosis as unprogrammed with cellular integrity disrupted via diverse, seemingly random events. More recently programmed modes of necrosis have been identified. Parthanatos reflects cell death associated with activation of poly(ADP ribose)polymerase-1 (PARP-1) (16). In necroptosis, tumor necrosis factor alpha (TNF-α) typically activates Receptor-interacting protein kinase 1 (RIPK1) (17). Apoptosis is linked to a series of caspases (18–20). Autophagy is a process wherein cells degrade diverse metabolic products (21). Levine and associates (22, 23) delineated a mode of cell death uniquely associated with autophagy, which was designated "autosis." Understanding the relationship of cocaine toxicity to one or more of these signaling systems might afford novel strategies for treating cocaine toxicity.

Recently we showed that behavioral effects of cocaine reflect a signaling cascade associated with nitric oxide (NO) and glyceraldehyde-3-phosphate dehydrogenase (GAPDH) (24). Generation of NO is triggered by a variety of stimuli such as glutamate neurotransmission acting via its *N*-methyl-D-aspartate (NMDA) subtype receptors. The NO nitrosylates GAPDH at a critical cysteine, abolishing its catalytic activity but conferring upon it the ability to bind to the ubiquitin E3 ligase Siah1. Nitrosylated GAPDH associated with Siah1 translocates to the nucleus. With cytotoxic insults nitrosylated GAPDH in the nucleus activates the histone acetylating complex p300/CBP which leads to acetylation and activation of p53 with associated enhancement of transcriptional targets, such as PUMA and Bax, that mediate cell death (25, 26). By contrast, physiologic stimuli associated with neurotrophic actions such as brain-derived neurotrophic factor (BDNF) and nerve growth factor (NGF) lead to the nuclear GAPDH–Siah1 complex binding and degrading the histone-methylating enzyme SUV39H1 (27). The diminished histone methylation is associated with augmented histone acetylation with enhancement of cAMP response element-binding protein (CREB)-regulated genes that facilitate nerve outgrowth.

We described a signaling cascade in which the NO/GAPDH/Siah1 system accounts for behavioral stimulant effects of low doses of cocaine as well as neurotoxic actions of high doses (24). The lower doses of cocaine augment CREB genes, whereas higher, neurotoxic, doses activate the cytotoxic p53 system. Evidence that both stimulant and cytotoxic influences involve NO/GAPDH/Siah1 signaling is provided by the use of the drug CGP3466B, an extremely potent inhibitor of GAPDH nitrosylation as well as GAPDH-Siah1 binding, which prevents both the stimulant and neurotoxic actions of cocaine (24, 28).

Significance

Cocaine is one of the most abused drugs in modern society, with overdoses that are frequently lethal. Molecular mechanisms underlying its toxic actions have been obscure. The present study demonstrates that cocaine's cellular toxicity involves a signaling cascade that utilizes the gasotransmitter nitric oxide, which leads to autophagy, a cellular modification that can cause cell death. Thus, manipulations that impair nitric oxide signaling and autophagy diminish cytotoxic actions of cocaine. By contrast, alterations of apoptosis and other non-autophagic modes of cell death are ineffective. Therapies directed toward the autophagic process may be beneficial in treating cocaine neurotoxicity.

Author contributions: P.G., M.M.H., and S.H.S. designed research; P.G. and M.M.H. performed research; P.G. and M.M.H. analyzed data; and P.G., M.M.H., and S.H.S. wrote the paper.

Reviewers: R.S.D., Yale University School of Medicine; and E.J.N., Icahn School of Medicine at Mount Sinai.

The authors declare no conflict of interest.

[1]P.G. and M.M.H. contributed equally to this work.

[2]To whom correspondence should be addressed. Email: ssnyder@jhmi.edu.

This article contains supporting information online at www.pnas.org/lookup/suppl/doi:10.1073/pnas.1524860113/-/DCSupplemental.

In the present study, we explored cellular/molecular mechanisms that underlie the cytotoxicity of cocaine. We show that cocaine selectively elicits activation of autophagy, which uniquely mediates cocaine's cytotoxic actions.

Results

Cocaine Elicits Autophagy in Neuronal Systems. LC3 (microtubule-associated protein 1 light chain-3) is the mammalian homolog of the yeast protein Atg8, a well-characterized mediator of autophagy (29). Mammalian autophagy is associated with the lipidation of LC3-I via the addition of phosphatidylethanolamine to generate LC3-II (30, 31). Formation of LC3-II can be regarded as an important marker for autophagy (32).

Treatment of primary neuronal cerebrocortical cultures with cocaine markedly augments formation of LC3-II with a maximal sevenfold increase and half-maximal effects at 1 μM (Fig. 1 *A* and *B*). Bafilomycin facilitates monitoring autophagic flux by increasing the pH of lysosomes, which prevents degradation of autophagic vesicles and reduces variability (32). In the presence of bafilomycin, cocaine enhances levels of LC3-II (Fig. 1*C*). Because bafilomycin prevents degradation of autophagic vesicles, these findings rule out the possibility that cocaine acts by

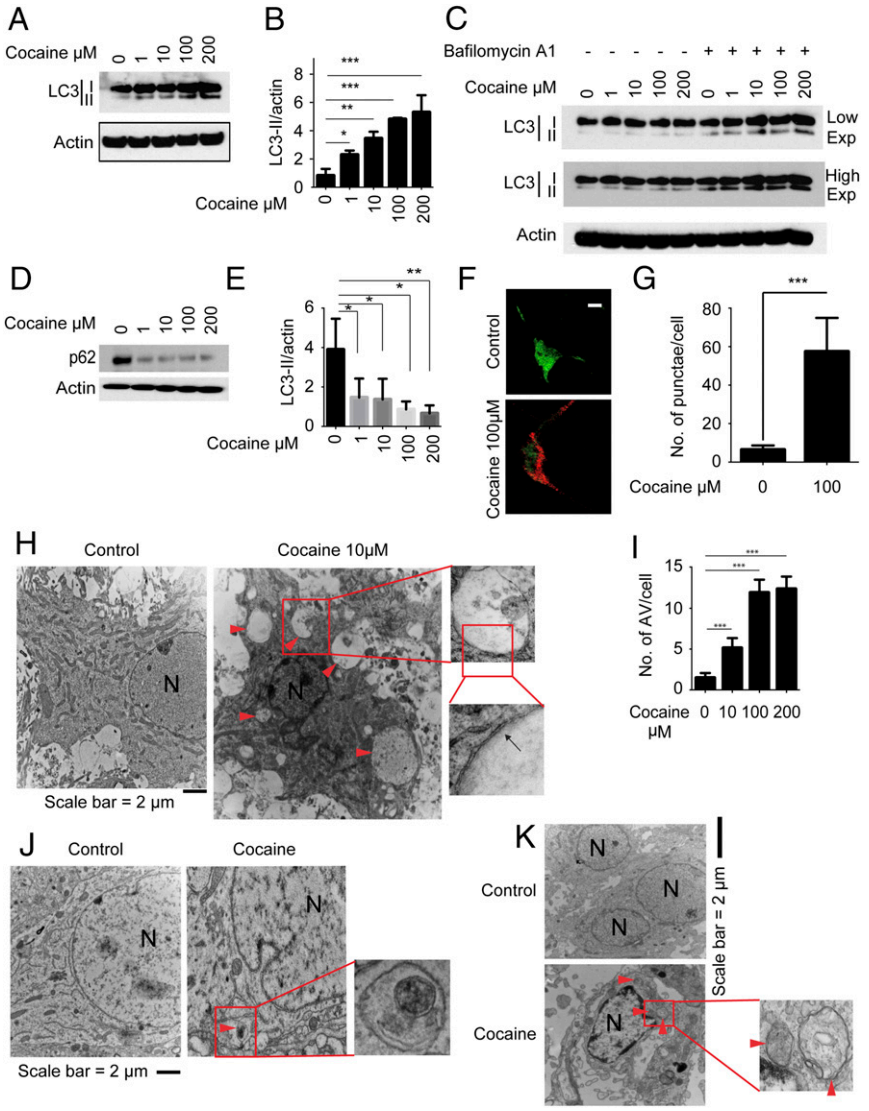

Fig. 1. Cocaine elicits autophagy in neuronal system. (*A* and *B*) Immunoblots and quantification assessing the protein levels of LC3-II in response to indicated concentrations of cocaine in cortical cultures ($n = 3$). (*C*) Immunoblot assessing the protein levels of LC3-II in response to indicated concentrations of cocaine ± 100 nM bafilomycin-A1. (*D*) Immunoblots assessing the protein levels of p62 in response to indicated concentrations of cocaine in cortical cultures. (*E*) Quantification of LC3-II protein levels in response to cocaine in cortical cultures ($n = 3$). (*F*) Confocal imaging of LC3 puncta (red) in cortical neurons ± 100 μM cocaine. Neuronal nuclei were stained green with NeuN antibody. (*G*) Quantification of LC3-II puncta per neuron ± cocaine treatment. A total of 50 neurons were counted. (Scale bar: 10 μm.) Data are represented as mean ± SD; $^{***}P < 0.001$, one-way ANOVA. (*H*) Transmission electron microscopy (TEM) images of cortical neurons with different indicated concentrations of cocaine for 3 h. Arrowhead represents autophagic vesicle, N denotes nucleus. (Scale bar: 2 μm.) The red boxed area contains a representative autophagic vacuole at 25,000× magnification. Arrow indicates double membrane of autophagic vacuole at 60,000× magnification. (*I*) Quantification of autophagic vacuoles per neuron ± cocaine. A total of 30 neurons were counted. Data are represented as mean ± SD; $^{***}P < 0.001$, $^{**}P < 0.01$, $^{*}P < 0.05$, one-way ANOVA. (*J*) TEM images of adult brain lateral habenula injected with vehicle or 20 mg/kg cocaine (intraperitoneal) for 3 h. (Scale bar: 2 μm.) The red boxed area contains a representative autophagic vacuole at 60,000× magnification. (*K*) TEM images of mouse fetal brain cerebral cortex. Timed pregnant mice were injected with vehicle or 20 mg/kg cocaine (intraperitoneal) for 3 h. (Scale bar: 2 μm.) The red boxed area contains representative autophagic vacuoles at 60,000× magnification.

altering the disposition of autophagic vesicles and establish that cocaine acts by increasing autophagy.

We also examined p62, an adaptor protein that binds to ubiquitylated proteins to facilitate their degradation via autophagy (32). In the process, p62 itself is degraded, with this degradation representing a marker for the autophagic process. Cocaine (1–200 μM) dramatically decreases protein levels of p62, which are virtually evident even at 1 μM dose of cocaine (Fig. 1*D*).

To assess autophagy at a morphologic level, we monitored LC3-II punctae by confocal microscopy (Fig. 1 *F* and *G*). We observed substantial increases in such punctae following cocaine treatment, further supporting autophagic actions of cocaine. Electron microscopic analysis of cortical cultures further supports the autophagic actions of cocaine (Fig. 1*H* and Fig. S1*A*). Numbers of autophagic vesicles are tripled by 10 μM cocaine and increased sixfold at 100/200 μM cocaine (Fig. 1*I*). Detailed morphologic examination reveals the double lamellar structure characteristic of autophagic vesicles.

We extended our analysis to intact mouse brain. Previous reports demonstrated neurotoxic effects of cocaine in the lateral habenula (33, 34). In brains of adult mice treated with cocaine, transmission electron microscopic analysis (TEM) reveals a substantial increase in numbers of autophagic vesicles in the lateral habenula (Fig. 1*J*). When pregnant mice were treated with cocaine, considerable numbers of autophagic vesicles are evident in the cerebral cortices of pups compared with pups of control pregnant mice (Fig. 1*K*).

To substantiate microscopic data, we performed Western blot analysis of LC3-II in different part of mice brain. As expected, treatment of cocaine substantially induced LC3-II level in dorsal striatum, cortex, lateral habenula, and nucleus accumbens compared with vehicle treated group. (Fig. S1 *B–E*).

In summary, multiple lines of evidence, both biochemical and morphologic, support an autophagic action of cocaine in neuronal systems.

Autophagic Actions of Cocaine Involve GAPDH Nitrosylation. Earlier, we reported that behavioral stimulant and neurotoxic actions of cocaine depend upon a signaling system involving NO nitrosylating GAPDH (24). Here we show that this process also underlies cocaine-associated autophagy.

In HEK-293 cells cocaine elicits autophagy monitored by the generation of LC3-II. Concentrations of 250 μM cocaine have been used, because HEK-293 cells are relatively insensitive to

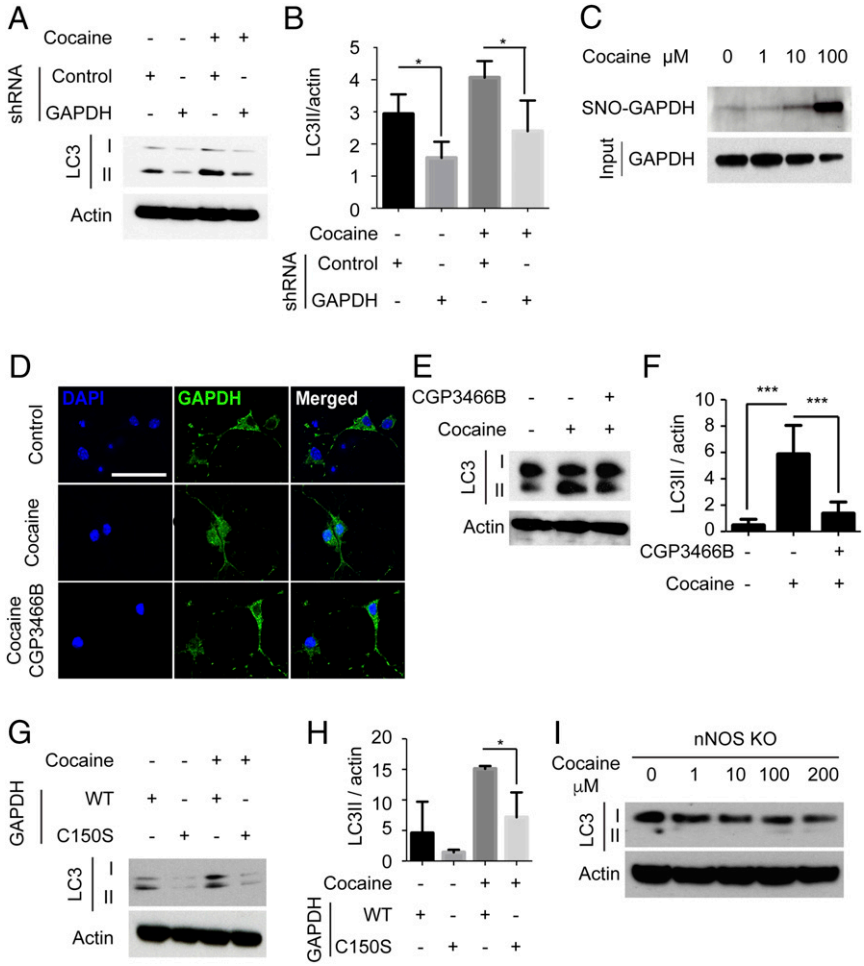

Fig. 2. Autophagic action of cocaine involves GAPDH nitrosylation. (*A* and *B*) Immunoblots and quantification of the protein levels of LC3-II in response to 250 μM cocaine in HEK-293 cells transfected with scrambled or GAPDH shRNA ($n = 3$). (*C*) Biotin switch assay for evaluating GAPDH nitrosylation in cortical cultures 5 min after cocaine treatment. (*D*) Confocal images of nuclear translocation of GAPDH (green) 5 min after 10 μM cocaine treatment in cortical neurons. Nuclei stained blue. (Scale bar: 50 μm.) (*E* and *F*) Immunoblots and quantification of the protein levels of LC3-II in response to 100 μM cocaine ± 2 nM CGP3466B in cortical cultures ($n = 3$). (*G* and *H*) Immunoblots and quantification of the protein levels of LC3-II in response to 250 μM cocaine after overexpressing wild-type HA-GAPDH or HA-C150S GAPDH mutant in HEK-293 cells ($n = 3$). (*I*) Immunoblots assessing the protein levels of LC3-II in response to cocaine in cortical cultures isolated from nNOS KO mice. The data are represented as mean ± SD; $^{***}P < 0.001$, $^{**}P < 0.01$, $^{*}P < 0.05$, one-way ANOVA.

autophagic actions of cocaine. Depletion of GAPDH by shRNA treatment (Fig. S2*A*) virtually abolishes the autophagic enhancement of LC3-II elicited by cocaine (Fig. 2 *A* and *B*).

Our previous study linking GAPDH nitrosylation to cocaine's actions used intact mice (24). In the present study, we evaluated cerebrocortical neuronal cultures, which differ notably from adult rodent brain in lacking the dopamine and serotonin neuronal systems that are classically involved in psychotropoic influences of cocaine. In these cultures, we demonstrate that cocaine (1–100 μM) elicits GAPDH nitrosylation (Fig. 2*C*) as well as nuclear translocation of GAPDH (Fig. 2*D*).

The NO/GAPDH/Siah1 system is potently inhibited by the drug CGP2466B, which, at very low nanomolar concentrations, prevents GAPDH nitrosylation (28). The cocaine-elicited augmentation of LC3-II is prevented by treatment with 2 nM CGP3466B (Fig. 2 *E* and *F*). Thus, GAPDH nitrosylation appears to be required for these actions of cocaine.

The nitrosylation of GAPDH that mediates the NO/GAPDH/Siah1 signaling system selectively involves C150 of GAPDH (25). We evaluated autophagic influences of cocaine in HEK-293 cells overexpressing wild-type GAPDH or GAPDH with cysteine-150 mutated to serine (GAPDH-C150S). Generation of LC3-II is evident after GAPDH over expression and appears to be significantly high after cocaine treatment compared with GAPDH-C150S mutant. The diminished autophagy is evident in the absence as well as the presence of cocaine (Fig. 2 *G*, *H*).

Next, we treated nNOS knockout (KO) mice-derived cortical cultures (Fig. S2*B*) to further confirm the role of NO in cocaine-induced autophagy. Increasing concentrations of cocaine failed to augment LC3-II levels in nNOS KO neurons (Fig. 2*I*).

These findings emphasize the importance of GAPDH nitrosylation in cocaine-induced autophagy in neurons.

Selectivity of Cocaine's Influences on Autophagic Neuronal Cell Death. Thus far, we have established that cocaine impacts autophagy. We next explored cocaine's actions upon other modes of programmed cell death. In neuronal cultures, cocaine half maximally elicits cell death at about 10 μM (Fig. 3*A*), which is prevented by CGP3466B (2 nM). We compared agents that influence different modes of cell death. The PARP-1–specific inhibitor, 3,4-dihydro-5-(4-(1-piperidinyl)butoxyl)-1(2H)-isoquinolinone (DPQ), selectively prevents parthanatos associated with PARP-mediated necrosis (35). Necrostatin uniquely blocks necroptosis, which is mediated by RIPK1 (17). *N*-benzyloxycarbonyl-Val-Ala-Asp-fluoromethylketone (Z-VAD-fmk) is a well characterized inhibitor of multiple caspases, a classical mediator of apoptosis (36). Cocaine-elicited cell death in cortical cultures is not significantly influenced by the inhibitors of parthanatos, necroptosis, and caspases (Fig. 3*B*). By contrast, bafilomycin (50 nM) abolishes cocaine-mediated cell death. Thus, cocaine-associated cell death can be attributed to autophagy rather than to other well known forms of programmed cell death.

To examine directly a selective role for autophagy in cocaine-associated cell death, we depleted either ATG 5 or beclin-1 (Fig. S3 *A* and *E*), physiologic mediators of autophagy (37). ATG 5 or beclin-1 depletion markedly diminishes cocaine cytotoxicity. By contrast, depletion of caspase-3, PARP-1, or RIPK1 (Fig. 3*C* and Fig. S3 *B*–*D*) has no influence upon the process. Apoptosis is selectively enhanced by staurosporine, a well known inhibitor of protein kinases (38). We examined the influence of staurosporine upon apoptosis monitored by cleavage of caspase-3 (39). Caspase-3 cleavage is elicited by staurosporine, but not by cocaine, indicating that cocaine does not display proapoptotic influences (Fig. 3*D*).

The DNA-alkylating agent MNNG elicits parthanatos-mediated cell death via PARP-1 cleavage (40). Whereas MNNG substantially cleaves PARP-1, cocaine fails to do so, indicating that cocaine does not act via parthanotos (Fig. 3*E*).

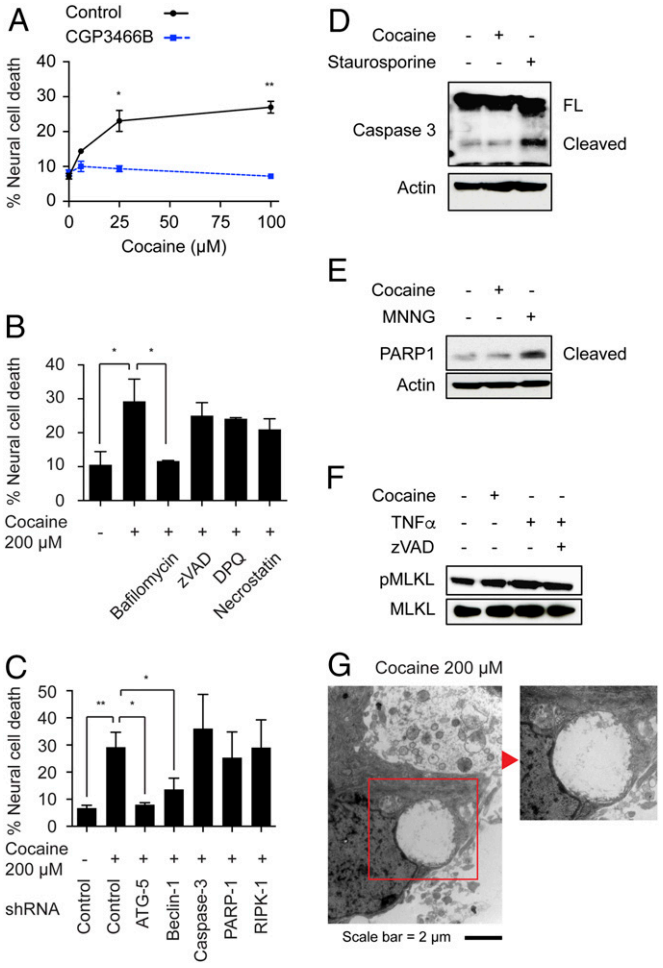

Fig. 3. Selectivity of cocaine's influence on autophagic neuronal cell death. The data are represented as mean ± SEM. (*A*) Effects of 2 nM CGP3466B on cell death of cortical neurons treated with indicated concentrations of cocaine. $*P < 0.05$, $**P < 0.01$, two-tailed *t* test. (*B*) Effects of different inhibitors on neuronal cell death at respective concentrations (50 nM bafilomycin, 30 μM DPQ, 30 μM necrostatin, 100 μM z-VAD) on cortical neurons treated with 200 μM cocaine. $*P < 0.05$, two-tailed *t* test. (*C*) Effects of ATG5 shRNA, Beclin-1 shRNA, PARP-1 shRNA, RIPK1 shRNA, and caspase-3 shRNA on cell death of cortical neurons treated with 200 μM cocaine. $*P < 0.05$, $**P < 0.01$, one-tailed *t* test. (*D*) Immunoblots assessing the protein levels of cleaved caspase-3 in response to 200 μM cocaine overnight, and 1 μM staurosporine for 4 h. (*E*) Immunoblots assessing the protein levels of cleaved PARP-1 in response to 200 μM cocaine overnight, and 500 μM MNNG for 4 h. (*F*) Immunoblots assessing the protein levels of phospho-MLKL in response to 200 μM cocaine overnight, 10 ng/mL TNF-α and 100 μM z-VAD for 4 h. (*G*) TEM images of primary cortical neurons treated with 200 μM cocaine overnight at 8,000× magnification. (Scale bar: 2 μm.) Red boxed areas show concave nucleus at 25,000× and 60,000× magnification.

MLKL is phosphorylated by RIPK1 in response to agents that stimulate necroptosis (41). Necroptosis is typically induced by treatment with TNF-α in the presence of Z-VAD-fmk, an apoptosis inhibitor (36). As reported previously (42), TNF-α, combined with Z-VAD-fmk, increases levels of phospho-MLKL. By contrast, cocaine has no influence, indicating that cocaine is not a stimulant of necroptosis (Fig. 3*F*).

Autophagic cell death is associated with specific morphologic alterations, such as nuclear concavity and swelling of the perinuclear space (22). Electron microscopic analysis reveals concavity of the nucleus following cocaine treatment (Fig. 3*G*). By contrast, we fail to observe nuclear fragmentation or membrane disruptions that characterize nonautophagic forms of cell death.

Discussion

Autophagic cell death is a relatively recently appreciated but well accepted phenomenon defined by specific criteria. Autophagic death is characterized by autophagic flux and the involvement of at least two autophagic regulatory factors along with the absence of apoptosis (43). Cocaine-elicited cell death fulfills these criteria. Thus, cocaine elicits autophagy as evaluated by several indices: induction of LC3-II, degradation of p62, ultrastructural analysis by TEM, and confocal monitoring of LC3 punctae. Moreover, we have ruled out involvement of cocaine in other modes of programmed cell death such as apoptosis, parthanatos, and necroptosis.

Cocaine induces autophagy in cortical cultures at concentrations as low as 1 μM. These levels are clinically relevant because recreational abuse of cocaine is associated with peak serum concentrations between 0.5 and 5 μM. The highest reported cocaine serum concentration in a living person is 120 μM. Cocaine concentrations in the brain are generally higher than those in the blood (44). In human toxicity cases, average brain-to-blood cocaine concentrations ratio is 9.6-fold (45).

Recently, other workers have described autophagy associated with cocaine. Guo et al. (46) reported activation of microglia in response to cocaine, which appeared to involve autophagy and inflammatory reactions. Cao et al. (37) detected autophagy in astrocytic cultures following treatment with cocaine. These studies were restricted to single cell lines and did not discriminate autophagy from other modes of cytotoxicity. By contrast, our study systematically rules out a variety of modes of programmed cell death and establishes that cocaine's toxic actions are uniquely associated with autophagy.

Our study also demonstrates that cocaine's impact upon autophagy involves the NO/GAPDH signaling cascade. Our earlier investigation (24) established a role for the NO/GAPDH system in cell death but failed to delineate the type of cell death involved. In this context, the effects of stimulant and neurotoxic doses of cocaine on NO/GAPDH signaling are blocked by dopamine D1 receptor inhibition. In the current work, cocaine induces NO/GAPDH signaling in primary cortical cultures, which lack the dopaminergic system. This information suggests the existence of another mechanism by which cocaine induces autophagy via the NO/GAPDH cascade. Further work is needed to delineate the upstream molecular events that lead to NO/GAPDH signaling-mediated activation of autophagy in response to high doses of cocaine.

Our findings may have therapeutic relevance. Thus, the notion that cocaine toxicity is uniquely associated with autophagy implies that selective and potent inhibitors of autophagy may be therapeutic in treating cocaine users. Such interventions in the autophagic process may also benefit infants born of cocaine-using mothers.

In terms of specific agents that might be beneficial, our observations that the NO/GAPDH pathway mediates cocaine actions may have therapeutic ramifications. CGP3466B prevents GAPDH nitrosylation at concentrations as low as 0.1 nM (28) and has been administered in clinical trials of patients with Parkinson's disease as well as amyotrophic lateral sclerosis (47, 48). In these studies CGP3466B appeared to be safe with negligible side effects. This drug or related agents may be beneficial in the therapy of cocaine abuse.

Materials and Methods

Reagents. Neurobasal-A medium (no glucose, no sodium pyruvate), B-27 supplement, and B-27 supplement minus antioxidants were purchased from Life Technologies. Staurosporine, DPQ, Z-VAD-FMK, and Necrostatin-1 were purchased from Santa Cruz Biotachnology. Bafilomycin A1 was purchased from Cayman Chemical. CGP3466B was purchased from Tocris Bioscience. Caspase-3, PARP-1, RIPK1, Beclin-1, and ATG-5 shRNA (verified) lentiviral plasmid, cocaine hydrochloride and poly-l-ornithine hydrobromide were purchased from Sigma-Aldrich. Recombinant murine TNF-α was purchased from Peprotech. *N*-methyl-*N*-nitroso-N′-nitroguanidine (MNNG) was purchased from Chem Service.

Antibodies. Anti–GAPDH-HRP was purchased from GenScript USA. Anti–MLKL, anti–phospho-MLKL, anti–caspase-3, anti-PARP-1, anti-nNOS, and anti-LC3 were purchased from Cell Signaling Technology. Anti-NeuN was purchased from EMD Millipore.

Transfections. HEK-293 cells transfections were performed using the polyfect transfection reagent following the manufacturer's instructions (Qiagen).

Lentivirus Production. Second-generation lentiviral vector packaging was used for lentivirus production. Lentiviral plasmids expressing caspase-3, PARP-1, RIPK-1, beclin-1, or ATG-5 shRNA were cotransfected into HEK-293T cells with packaging system psPAX2 and pMD2 plasmids. The media was changed after overnight incubation. The lentivirus-containing supernatant was collected after 48 h. Floating cells and cell debris were pelleted by centrifugation of the supernatant at 2,000 × *g* for 10 min at 4 °C. Lentivirus particles were pelleted by ultracentrifugation at 100,000 × *g* for 2 h at 4 °C. The lentiviral pellet was resuspended in 1/200th volume of OPTI-MEM and stored in −80 °C until use.

Primary Neuron Cultures. Animals were housed and cared for in accordance with the National Institutes of Health *Guide for the Care and Use of Laboratory* (49). Animal experiments were approved by the Johns Hopkins University Animal Care and Use Committee (JHU ACUC). Mouse primary cortical cultures were prepared from gestational day 16–18 fetal CD-1 mice. Briefly, the timed pregnant mice were killed by decapitation, the uterus was quickly dissected out, and pups were decapitated. After removing meninges, the cerebral cortices were dissected and incubated in 0.025% trypsin–EDTA solution for 15 min. The cells were triturated in plating media containing Neurobasal-A media without glucose and sodium pyruvate supplemented with 12.5 mM glucose, 2 mM L-glutamine, and 2% (vol/vol) B-27 minus antioxidants. The cortical cultures were plated on poly-L-ornithine coated plates.

Cortical Culture Treatment. Primary cortical cultures were used between day in vitro (DIV) 10 and DIV 15. Half of the media was removed from the cells, mixed with 2× the indicated concentrations of reagents, whereupon the media was returned to the cells. Cultures were incubated in cocaine-containing media for 3 or 48 h, respectively, in autophagy and cell death experiments.

Cell Death Assay. Live cultures were stained 48 h after cocaine treatment with 1 μg/mL Hoechst 33342, which stains all cell nuclei, and 7 μM propidium iodide, which stains dead cell nuclei. Images were immediately collected using Carl Zeiss Axiovert 200M microscope. Quantification of cell death in neurons was performed using NIH image-J software. Neuronal nuclei are smaller in size and fluoresce at a significantly higher intensity than glial nuclei. Using these criteria, only neuronal nuclei were counted.

Biotin Switch Assay. Primary cortical cultures were lysed on ice in lysis buffer containing 100 mM Hepes, 1 mM EDTA, 0.1 mM neocuproine, pH 8.0, 1% SDS, 1% Nonidet P-40, and 100 mM sodium chloride. DNA was degraded by passing lysate through a 27 gauge needle several times on ice. For each reaction 1 mg of total protein was used. Free thiols in denatured lysates were blocked with methyl methanethiosulfonate (MMTS) at 50 °C for 20 min. MMTS was removed by acetone precipitation. Nitrosylated thiols were reduced using sodium ascorbate and then biotinylated. Streptavidin beads were used to pull down proteins bearing biotinylated thiols for further evaluation by Western blot analysis.

Confocal Imaging of Neuronal Nuclei and LC3 Punctae in Neurons. Cortical neurons were transduced with LC3-RFP using LentiBrite RFP-LC3 Lentiviral Biosensor (Millipore) to image LC3 puncta. For immunostaining, cells were fixed with 4% (wt/vol) paraformaldehyde, permeabilized with 0.3% Triton X-100, and blocked with 5% (vol/vol) goat serum. Mouse anti-NeuN antibody was used at a dilution of 1:100 in 0.025% goat serum in PBS overnight at 4 °C. For GAPDH immunostaining, GAPDH antibody was used at a dilution of 1:500. GAPDH immunostaining, LC3 puncta, and neuronal nuclei were imaged under Zeiss Axiovert 200 with 510-Meta confocal module. Images were collected using a 40× (oil) 1.3 NA Zeiss Plan-Neofluar objective. Number of LC3 puncta per cell were counted using Imaris software version 7.7.2.

Transmission Electron Microscopy (TEM). Primary cortical neurons were treated with indicated concentrations of cocaine. The cells were fixed in 2.5% (vol/vol)

glutaraldehyde, 3 mM $MgCl_2$, in 0.1 M sodium cacodylate buffer, pH 7.2, for 1 h at room temperature. After buffer rinse, samples were postfixed in 1% osmium tetroxide in buffer (1 h) on ice in the dark. The cells were stained with 2% (wt/vol) aqueous uranyl acetate (0.22 μm filtered, 1 h in the dark), dehydrated in a graded series of ethanol solutions, and embedded in Eponate 12 (Ted Pella) resin. Samples were polymerized at 37 °C for 2–3 d before moving to 60 °C overnight.

Brain Tissue Preparation for TEM. Mice were perfused with 2% (wt/vol) paraformaldehyde (freshly prepared from EM grade prill form), 2% (vol/vol) glutaraldehyde, 3 mM $MgCl_2$, in 0.1 M sodium cacodylate buffer, pH 7.2, for 30 min at a rate of 2 mL/min, then postfixed overnight. Regions of interest were dissected and samples were washed in 0.1 M sodium cacodylate buffer with 3 mM $MgCl_2$ and 3% (wt/vol) sucrose. Samples were postfixed in reduced 2% (wt/vol) osmium tetroxide, 1.6% (wt/vol) potassium ferrocyanide in buffer (2 h) on ice in the dark. Samples were stained with 2% (wt/vol) aqueous uranyl acetate (0.22 μm filtered, 1 h in the dark), dehydrated in a graded series of ethanol propylene oxide solutions, and embedded in Eponate 12 (Ted Pella) resin. Samples were polymerized at 60 °C overnight. Thin sections (60–90 nm) were cut with a diamond knife on a Reichert-Jung Ultracut E ultramicrotome and picked up with 2 × 1 mm copper slot grids. Grids were stained with 2% (wt/vol) uranyl acetate in 50% (vol/vol) methanol and lead citrate at 4 °C and observed with a Hitachi 7600 TEM. Images were captured with an AMT CCD XR50 (2K × 2K) camera.

Western Blot Analysis. Cell lysates were prepared using lysis buffer (150 mM NaCl, 0.5% CHAPS, 0.1% Triton, 0.1% BSA, 1 mM EDTA, protease inhibitors, phosphatase inhibitors). Samples were centrifuged at 14,000 × *g* for 20 min, and the protein concentration of the supernatant was measured (Bio-Rad Protein Assay Dye Reagent Concentrate). Proteins were resolved by SDS-polyacrylamide gel electrophoresis and transferred to PVDF membranes. The membranes were blocked for 2 h at room temperature in 20 mM Tris·HCl, pH 7.4, 150 mM NaCl, and 0.02% Tween 20 (Tris-buffered saline/Tween 20) containing 3% (wt/vol) BSA followed by overnight incubation at 4 °C in 1:1,000 dilution of the respective antibodies for LC3, p62, actin, GAPDH, MLKLp, MLKL, caspase 3, PARP, beclin-1, ATG5, and RIPK in 3% (wt/vol) BSA. The membrane was washed three times with Tris-buffered saline/Tween 20, incubated with HRP-conjugated secondary antibody, and the bands visualized by chemiluminescence. The depicted blots are representative replicates selected from at least three experiments.

Western Blot Image Quantification and Statistical Analysis. Western blot images were quantified using ImageJ software. Data are presented as means ± SD. Unless otherwise indicated, statistical analysis was performed using Graphpad software with an alpha power level of 0.05. Two-tailed *t* test was used to perform two group comparisons. One-way analysis of variance (ANOVA) was used to perform multiple comparisons. Data were graphed as means ± SEM.

ACKNOWLEDGMENTS. We thank Barbara Smith (TEM specialist at Johns Hopkins School of Medicine) for her help in preparation of TEM samples. This work was supported by National Institutes of Health/National Institute on Drug Abuse Grant DA000266.

1. Whitby LG, Hertting G, Axelrod J (1960) Effect of cocaine on the disposition of noradrenaline labelled with tritium. *Nature* 187:604–605.
2. Pradhan SN, Battacharyya AK, Pradhan S (1978) Serotoninergic manipulation of the behavioral effects of cocaine in rats. *Commun Psychopharmacol* 2(6):481–486.
3. Axelrod J (1971) Noradrenaline: Fate and control of its biosynthesis. *Science* 173(3997): 598–606.
4. Ritz MC, Lamb RJ, Goldberg SR, Kuhar MJ (1987) Cocaine receptors on dopamine transporters are related to self-administration of cocaine. *Science* 237(4819): 1219–1223.
5. Carlezon WA, Jr, et al. (1998) Regulation of cocaine reward by CREB. *Science* 282(5397):2272–2275.
6. Nestler EJ (2005) The neurobiology of cocaine addiction. *Sci Pract Perspect* 3(1):4–10.
7. Kelz MB, et al. (1999) Expression of the transcription factor deltaFosB in the brain controls sensitivity to cocaine. *Nature* 401(6750):272–276.
8. Kennedy PJ, et al. (2013) Class I HDAC inhibition blocks cocaine-induced plasticity by targeted changes in histone methylation. *Nat Neurosci* 16(4):434–440.
9. Covington HE, 3rd, et al. (2011) A role for repressive histone methylation in cocaine-induced vulnerability to stress. *Neuron* 71(4):656–670.
10. Maze I, et al. (2010) Essential role of the histone methyltransferase G9a in cocaine-induced plasticity. *Science* 327(5962):213–216.
11. Renthal W, et al. (2009) Genome-wide analysis of chromatin regulation by cocaine reveals a role for sirtuins. *Neuron* 62(3):335–348.
12. Kumar A, et al. (2005) Chromatin remodeling is a key mechanism underlying cocaine-induced plasticity in striatum. *Neuron* 48(2):303–314.
13. Galluzzi L, et al. (2015) Essential versus accessory aspects of cell death: Recommendations of the NCCD 2015. *Cell Death Differ* 22(1):58–73.
14. Kerr JF (1971) Shrinkage necrosis: A distinct mode of cellular death. *J Pathol* 105(1): 13–20.
15. Kerr JF, Wyllie AH, Currie AR (1972) Apoptosis: A basic biological phenomenon with wide-ranging implications in tissue kinetics. *Br J Cancer* 26(4):239–257.
16. Andrabi SA, et al. (2006) Poly(ADP-ribose) (PAR) polymer is a death signal. *Proc Natl Acad Sci USA* 103(48):18308–18313.
17. Degterev A, et al. (2005) Chemical inhibitor of nonapoptotic cell death with therapeutic potential for ischemic brain injury. *Nat Chem Biol* 1(2):112–119.
18. Nicholson DW, et al. (1995) Identification and inhibition of the ICE/CED-3 protease necessary for mammalian apoptosis. *Nature* 376(6535):37–43.
19. Pronk GJ, Ramer K, Amiri P, Williams LT (1996) Requirement of an ICE-like protease for induction of apoptosis and ceramide generation by REAPER. *Science* 271(5250): 808–810.
20. Xue D, Horvitz HR (1995) Inhibition of the Caenorhabditis elegans cell-death protease CED-3 by a CED-3 cleavage site in baculovirus p35 protein. *Nature* 377(6546):248–251.
21. Kaur J, Debnath J (2015) Autophagy at the crossroads of catabolism and anabolism. *Nat Rev Mol Cell Biol* 16(8):461–472.
22. Liu Y, et al. (2013) Autosis is a Na+,K+-ATPase-regulated form of cell death triggered by autophagy-inducing peptides, starvation, and hypoxia-ischemia. *Proc Natl Acad Sci USA* 110(51):20364–20371.
23. Liu Y, Levine B (2015) Autosis and autophagic cell death: The dark side of autophagy. *Cell Death Differ* 22(3):367–376.
24. Xu R, et al. (2013) Behavioral effects of cocaine mediated by nitric oxide-GAPDH transcriptional signaling. *Neuron* 78(4):623–630.
25. Hara MR, et al. (2005) S-nitrosylated GAPDH initiates apoptotic cell death by nuclear translocation following Siah1 binding. *Nat Cell Biol* 7(7):665–674.
26. Sen N, et al. (2008) Nitric oxide-induced nuclear GAPDH activates p300/CBP and mediates apoptosis. *Nat Cell Biol* 10(7):866–873.
27. Sen N, Snyder SH (2011) Neurotrophin-mediated degradation of histone methyltransferase by S-nitrosylation cascade regulates neuronal differentiation. *Proc Natl Acad Sci USA* 108(50):20178–20183.
28. Hara MR, et al. (2006) Neuroprotection by pharmacologic blockade of the GAPDH death cascade. *Proc Natl Acad Sci USA* 103(10):3887–3889.
29. Klionsky DJ, et al. (2012) Guidelines for the use and interpretation of assays for monitoring autophagy. *Autophagy* 8(4):445–544.
30. Tanida I, Ueno T, Kominami E (2008) LC3 and Autophagy. *Methods Mol Biol* 445: 77–88.
31. Fader CM, Colombo MI (2009) Autophagy and multivesicular bodies: Two closely related partners. *Cell Death Differ* 16(1):70–78.
32. Mizushima N, Yoshimori T, Levine B (2010) Methods in mammalian autophagy research. *Cell* 140(3):313–326.
33. Ellison G (1992) Continuous amphetamine and cocaine have similar neurotoxic effects in lateral habenular nucleus and fasciculus retroflexus. *Brain Res* 598(1-2):353–356.
34. Murphy CA, Ghazi L, Kokabi A, Ellison G (1999) Prenatal cocaine produces signs of neurodegeneration in the lateral habenula. *Brain Res* 851(1-2):175–182.
35. Yu SW, et al. (2002) Mediation of poly(ADP-ribose) polymerase-1-dependent cell death by apoptosis-inducing factor. *Science* 297(5579):259–263.
36. Slee EA, et al. (1996) Benzyloxycarbonyl-val-ala-asp (OMe) fluoromethylketone (Z-VAD.FMK) inhibits apoptosis by blocking the processing of CPP32. *Biochem J* 315(Pt 1):21–24.
37. Russell RC, et al. (2013) ULK1 induces autophagy by phosphorylating Beclin-1 and activating VPS34 lipid kinase. *Nat Cell Biol* 15(7):741–750.
38. Falcieri E, Martelli AM, Bareggi R, Cataldi A, Cocco L (1993) The protein kinase inhibitor staurosporine induces morphological changes typical of apoptosis in MOLT-4 cells without concomitant DNA fragmentation. *Biochem Biophys Res Commun* 193(1): 19–25.
39. Kothakota S, et al. (1997) Caspase-3-generated fragment of gelsolin: Effector of morphological change in apoptosis. *Science* 278(5336):294–298.
40. Kang HC, et al. (2011) Iduna is a poly(ADP-ribose) (PAR)-dependent E3 ubiquitin ligase that regulates DNA damage. *Proc Natl Acad Sci USA* 108(34):14103–14108.
41. Cai Z, et al. (2014) Plasma membrane translocation of trimerized MLKL protein is required for TNF-induced necroptosis. *Nat Cell Biol* 16(1):55–65.
42. Sawai H (2013) Differential effects of caspase inhibitors on TNF-induced necroptosis. *Biochem Biophys Res Commun* 432(3):451–455.
43. Galluzzi L, et al. (2012) Molecular definitions of cell death subroutines: Recommendations of the Nomenclature Committee on Cell Death 2012. *Cell Death Differ* 19(1): 107–120.
44. Heard K, Palmer R, Zahniser NR (2008) Mechanisms of acute cocaine toxicity. *Open Pharmacol J* 2(9):70–78.
45. Spiehler VR, Reed D (1985) Brain concentrations of cocaine and benzoylecgonine in fatal cases. *J Forensic Sci* 30(4):1003–1011.
46. Guo ML, et al. (2015) Cocaine-mediated microglial activation involves the ER stress-autophagy axis. *Autophagy* 11(7):995–1009.
47. Olanow CW, et al. (2006) TCH346 as a neuroprotective drug in Parkinson's disease: A double-blind, randomised, controlled trial. *Lancet Neurol* 5(12):1013–1020.
48. Miller R, et al.; TCH346 Study Group (2007) Phase II/III randomized trial of TCH346 in patients with ALS. *Neurology* 69(8):776–784.
49. Committee on Care and Use of Laboratory Animals (1996) *Guide for the Care and Use of Laboratory Animals* (Natl Inst Health, Bethesda), DHHS Publ. No. (NIH) 85-23.